Determining the hydronium pK_a at platinum surfaces and the effect on pH-dependent hydrogen evolution reaction kinetics

Guangyan Zhong^{a,1}, Tao Cheng^{b,c,1}, Aamir Hassan Shah^a, Chengzhang Wan^a, Zhihong Huang^d, Sibo Wang^a, Tianle Leng^c, Yu Huang^{d,e,2}, William A. Goddard III^{c,f,2}, and Xiangfeng Duan^{a,e,2}

^aDepartment of Chemistry and Biochemistry, University of California, Los Angeles, California 90095, USA; ^bInstitute of Functional Nano & Soft Materials (FUNSOM), Jiangsu Key Laboratory for Carbon-Based Functional Materials & Devices, Joint International Research Laboratory of Carbon-Based Functional Materials and Devices, Soochow University; Suzhou, 215123, Jiangsu, PR China; ^cMaterials and Process Simulation Center (MSC), California Institute of Technology, Pasadena, California 191125, USA; ^dDepartment of Materials Science and Engineering, University of California; Los Angeles, California 90095, USA; ^cCalifornia NanoSystems Institute, University of California; Los Angeles, Los Angeles, California 90125, USA; ^cCalifornia 91125, USA

This manuscript was compiled on August 11, 2022

10

11

12

13

Electrocatalytic hydrogen evolution reaction (HER) is critical for green hydrogen generation and exhibits a distinct pH-dependent kinetics that has been elusive to understand. A molecular level understanding of the electrochemical interfaces is essential for developing more efficient electrochemical processes. Here we exploit an exclusively surface-specific electrical transport spectroscopy (ETS) approach to probe the Pt-surface water protonation status and experimentally determine the surface hydronium pK_a=4.3. Quantum mechanics (QM) and ReaxFF molecular dynamics (RMD) calculations confirm the enrichment of hydroniums (H₃O^{+*}) near Pt-surface and predict a surface hydronium pK_a of 2.5-4.4, corroborating the experimental results. Importantly, the observed Pt-surface hydronium pK_a correlates well with the pH-dependent HER kinetics, with the protonated surface state at lower pH favoring fast Tafel kinetics with a Tafel slope of 30 mV/decade, and the deprotonated surface state at higher pH following Volmer-step limited kinetics with a much higher Tafel slope of 120 mV/decade, offering a robust and precise interpretation of the pH-dependent HER kinetics. These insights may help design improved electrocatalysts for renewable energy conversion.

Electrochemical Reaction | Electrode/Electrolyte Interface | Multiscale Modeling | ...

Platinum (Pt) group metal catalysts play an essential role in electrochemical energy conversion and storage, a field of central importance to the advancement of various renewable energy technologies (1–3). A fundamental understanding of the molecular structures of the electrochemical interfaces and their role in governing the heterogeneous electrocatalytic reaction rates is essential for developing the future generation of electrocatalysts with improved catalytic activity and stability for various electrochemical processes, including electrocatalytic hydrogen evolution reactions (HER) critical for renewable chemical fuel generation (4–6). To this end, various in situ characterizations have been applied, including X-ray based spectroscopy, vibrational spectroscopies including Fourier transform infrared (FTIR), sum-frequency generation (SFG), and Raman spectroscopy (7–12).

Despite pioneering spectroscopic investigations, it remains uncertain how the bulk environment, including solution pH and electrode potential, affects the density/distribution of hydroniums near the catalytic surface, how the hydroniums interacting directly with the Pt electrode affect the interfacial molecular structure, and the role they play in electrochemical reactions. Direct and specific interrogation of the interfacial

charge and atom transfer process and their correlation with theoretical modeling has been a persistent challenge even for the most basic electrochemical processes. For example, although Pt-catalyzed HER involves only $2e^-$ transfer, representing a prototype electrochemical reaction model for investigating and establishing many basic concepts in electrochemistry, the nature of the catalytically active sites on Pt nanocatalysts and the origin of the distinct pH-dependent kinetics remains hotly debated (13–15). Studies and interpretations to date are often based on the bulk solution environment or the continuum concepts of the electrochemical double layer (EDL), while the exact molecular structure at the catalyst surface where the actual actions occur remains elusive.

27

31

32

33

34

37

38

39

40

41

42

43

In particular, the interfacial water plays a central role in forming the EDL, determining solute/electrode association, and mediating electron transfer (ET), proton transfer (PT), and proton-coupled electron transfer (PCET). The central role of water in aqueous phase electrochemistry is recently generating substantial interest (5, 16), but has not yet been sufficiently characterized. For example, Koper et al. attributed the pH-dependent HER activity to the interfacial water structure: i.e. how far the electrode potential is with respect to the

Significance Statement

Electrocatalytic hydrogen evolution reaction (HER) exhibits distinct pH-dependent kinetics that has been elusive to understand. Understanding the electrochemical interfaces is essential for developing more efficient electrochemical processes. In this research, we combine experiment and theory to establish a molecular-level understanding of the electrochemical interfaces. An exclusively surface-specific electrical transport spectroscopy approach probes the Pt-surface water protonation status and experimentally determines the surface hydronium pK $_{\alpha}$ =4.3. These insights offer a molecular-level interpretation of pH-dependent HER kinetics and may help design improved electrocatalysts for renewable energy conversion.

X.D. conceived the project; G.Z. conducted the experiments with assistance from Z.H., C.W., A.H.S., S.W.; T.C. and T.L.L. conducted the calculations; Y.H., W.A.G. and X.D. supervised the project; G.Z., T.C., W.A.G. and X.D. wrote the paper with comments from all authors.

There are no conflicts to declare.

¹G.Y.Z. contributed equally to this work with T.C.

²To whom correspondence should be addressed. E-mail: yhuangseas.ucla.edu (Y.H.);wagcaltech.edu (W.A.G.); xduanchem.ucla.edu (X.F.D.)

potential of zero (free) charge (pzfc) (5). While the potential dependence of the interfacial water structure has been explored extensively, the effect of pH (especially in acidic conditions where hydronium dominates) is not well understood (17–19). Markovic and Chan independently attributed the decrease in HER activity at higher pH to a change in the proton donor from $\rm H_3O^+$ to $\rm H_2O$ (15, 19, 20). However, the molecular-level origin of this phenomenon and the precise switching point have not been fully elucidated.

Early studies investigated hydroniums on metal surfaces using an ultrahigh vacuum model where the effective electrode potential was controlled through co-adsorption of varying amounts of hydrogen with water on Pt(111) at 100 K (21). Using high-resolution electron energy loss spectroscopy (HREELS), Wagner and Moylan reported $\rm H_3O^+$ formation from H(ad) and $\rm H_2O(ad)$ coadsorbed on a Pt(111) (21). Hydronium ions coadsorbed with bisulfate anions were detected by infrared reflection absorption spectroscopy (IRAS) on Pt(111) (22, 23). More recently, surface-enhanced infrared absorption spectroscopic (SEIRAS) studies were reported to reveal the bending mode from hydronium adsorbed on the Au surface (24).

Meanwhile, atomistic molecular dynamics (MD) simulations using density functional theory (DFT) calculations have been developed to explore the complex interfacial molecular structures at electrode/electrolyte interfaces (EEI). In particular, the structures of hydronium/hydrated proton clusters at the metal/solution interface have been studied theoretically using DFT and reactive dynamics (25–29). Previous simulations have shown that the excess protons preferentially adsorb at the Pt-water interface (30, 31) or that hydroniums enrich near the Pt-water interface(32). These studies suggest that the Pt surface water molecules tend to prefer protonation compared to bulk water molecules. In other words, the Pt surface hydroniums (H_3O^+) exhibit a higher pK_a than bulk H_3O^+ far from the surface (p K_a =0). However, a direct experimental evaluation of the surface water protonation status and the surface hydronium pKa to validate such theoretical expectations has not been possible due to the lack of a surface-specific signal for the adsorbed $H_3\mathrm{O}^+$ and the complex convolution with near-surface or bulk water signals.

Here we report an electrical transport spectroscopy (ETS) approach that provides a highly surface-specific probe of the water structure on platinum nanowire (PtNW) surfaces (~ 2nm wide) under controlled potentials over a the pH range from 0 to 7. These ETS studies reveal a distinct pH dependent signal with a sharp switch at a critical point that closely resembles a typical titration curve. This pH-dependent switch in the ETS signal is well fitted by the classic Henderson–Hasselbalch equation, giving a $pK_a = 4.3$. This is the first quantitative confirmation that Pt-surface hydroniums exhibit a pK_a significantly above that of the bulk solution (p $K_a=0$). These experimental studies were corroborated with DFT-MD calculations on Pt(100) and Pt(111) surface as well as 10,000-atom ReaxFF reactive molecular dynamics (MD) simulations on the realistic PtNW structure (33). The multiscale simulation confirms the enrichment of $\mathrm{H_{3}O^{+}}$ near the Pt surface and predicts a surface hydronium pK_a of 2.5-4.4. Importantly, the observed surface hydronium pK_a correlates well with pH-dependent HER kinetics, where the protonated surface states at low pH (0-3) favor faster kinetics with a Tafel slope of 30 mV/decade (with $\rm H_3O^+$ as the proton supply and the Tafel reaction as the rate-limiting step), while the deprotonated states at high pH (5-7) show slower kinetics with a much higher Tafel slope of 120 mV/decade limited by the hydrogen adsorption step (with $\rm H_2O$ as the proton supply and the Volmer reaction as the rate-limiting step). This excellent correlation provides, for the first time, a robust interpretation of the pH-dependent HER kinetics on Pt surfaces. These studies make a critial step toward a more complete understanding of pH effects on the surface water structure and their critical role in the relevant electrochemical reactions and renewable energy conversion. (34)

Electrical Transport Spectroscopy (ETS) Probe of the Pt Surface Hydronium pK_a

Electrical transport spectroscopy (ETS) provides a concurrent measurement of electrical transport properties (e.g., conductance) and electrochemical behaviour of the catalyst materials at various electrochemical potentials (Fig. 1a). This ultrasensitive on-chip signaling technique provides critical information directly related to the dynamic surface states under controlled potentials (35, 36). By using a metallic Pt nanowire (PtNW) network, the ETS signal is exclusively specific to surface adsorbates and does not depend on long-range charge states. In general, electron transport in ultrafine PtNWs is sensitively dependent on the surface adsorbates that can produce different degrees of scattering of the conduction electrons depending on the exact molecular structure of the surface adsorbates and how they interact with PtNW surface (Fig. 1a, inset) (35–37).

Within the ETS approach, the electrical conductivity of ultrafine metallic PtNWs is sensitively dependent on the surface adsorbates due to surface adsorbate induced scattering of the conduction electrons, producing a resistance change following relationship:

$$\rho = \rho_0 \left(\left(\frac{1-p}{1+p} \right) \times \frac{\lambda}{d} \right) \qquad (d \leqslant \lambda)$$
 [1]

where ρ is the resistivity of the one-dimensional PtNWs and and ρ_0 is the resistivity of the bulk metal, λ is the electron mean free path, d is the PtNW diameter, and p is a specularity parameter with a value ranging from 0 (for highly diffusive scattering) to 1 (completely specular scattering). When the diameter (d) of the PtNWs is smaller than the electron mean free path ($\lambda \sim 5$ nm for Pt), the resistance is highly dependent on the exact surface adsorbate, which modifies the value of specularity (p).

Importantly, unlike semiconductor nanowires for which conductance may be affected by nearby charges or the electrochemical potential, the conductance of the metallic PtNWs is insensitive to nearby charge or electrochemical potential. For example, it has been shown previously that the conductance remains essentially constant at different potentials when the PtNW surface is covered with a stable surface adsorbate (e.g., CO or I⁻, see SI Appendix, Fig. S1 and ref (35, 36, 38)), confirming that the electrochemical potential and charge beyond the direct surface adsorbates has little direct effect on the conductance of the nanowire. Instead, when such stable surface adsorbates are removed, the conductance of the PtNWs shows notable dependence on electrochemical potential due to distinct surface adsorbates at different potentials. Thus, the

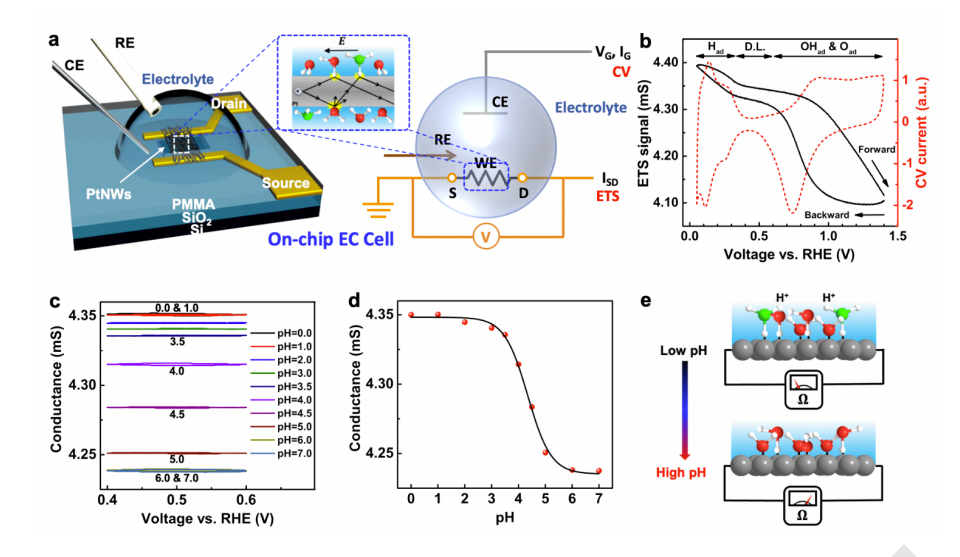


Fig. 1. In situ electrical transport spectroscopy (ETS) of hydronium adsorption on Pt surface. a, Schematic illustration of the on-chip electrochemical cell show ing polymethyl methacrylate (PMMA) covered gold electrodes and the exposed PtNWs in the opened PMMA window. Together with the diagram depicting working principles of concurrent CV and ETS. CE, counter electrode; RE, reference electrode; WE, working electrode; S, source; D, drain. The inset schematically illustrates the scattering (yellow star shape) of conduction electrons in the PtNWs by surface adsorbates. The red and white spheres represent O and H atoms of water molecules, while the oxygen atom of hydronium is green. b. Cyclic voltammetry and in-situ conductance vs. potential of the PtNWs in unbuffered solution at pH 1, showing a distinct hydrogen adsorption/desorption (Had) region; the double layer (D.L.) region, and the surface oxide formation/reduction region (OHad & Oad) as labeled. c, Conductance of a typical PtNW device under controlled potential at different pH. d, Conductance vs. pH relationship of a typical PtNW device over the range of pH = 0 to 7. The Black curve is a sigmoid fit of the conductance data based on the Henderson-Hasselbalch equation. e, Schematic model representing a structural change of surface water caused by hydronium ions.

202

204

205

206

207

208

210

211

212

213

214

215

216

217

218

219

220

221

222

223

224

226

227

228

229

230

231

232

233

234

235

236

237

238

ETS measurements with PtNWs provide a highly exclusive signal pathway to monitor the surface molecular adsorbates at electrode/electrolyte interfaces, with essentially no interference from the near-surface or bulk solution background.

165

166

167

168

169

170

171

172

173

174

175

176

177

178

180

181

182

183

185

186

187

188

189

190

191

192

193

194

195

196

197

198

199

200

201

We first compared typical cyclic voltammograms (CV) of the PtNWs with the measured ETS characteristics in unbuffered solutions of perchloric acid (HClO₄) with a pH value of 1 in the potential range of 0.05 V-1.40 V vs. the reversible hydrogen electrode (V_{RHE}) (Fig. 1b). The ETS measurements show a highly reproducible signal that matches well with the CV over the measured potential range, which can be roughly partitioned into three distinct surface adsorption regions:

- (1) the hydrogen adsorption-desorption region (0.05-0.35 V vs. V_{RHE}) where a higher ETS conductance signal is observed with increasing hydrogen adsorption toward lower potential;
- (2) the double layer region (0.35-0.60 vs. V_{RHE}) where the surface adsorption is dominated by water molecules and the ETS conductance shows only a moderate change with the potential:
- (3) the hydroxyl adsorption-desorption region (0.60-1.00 vs. V_{RHE}) and the Pt-oxide region (1.00-1.40 vs. V_{RHE}) where the surface is dominated by hydroxyl adsorption and surface oxide, with substantially increased surface scattering and reduced conductance.

While it is straightforward to understand the increased conductance of the PtNWs in the hydrogen adsorption region due to reduced scattering by surface H-adsorption (39), and the decreased conductance in the higher potential region due to surface oxidation, it is intriguing that we observe a small slope in the double layer region where surface adsorption is dominated by water molecules. In the double-layer region, we should expect a flat ETS signal (no conductance change with varying potential) since water molecules remain the dominant surface adsorbates with no apparent redox surface adsorption in this potential range. Nonetheless, a clear slope is observed in the ETS signal in this regime (Fig. 1 b), which might be attributed to a slight reaction hysteresis: including residue redox

processes [e.g., continued oxidation of incompletely desorbed H in the forward (positive) scan or continued reduction of the incompletely reduced hydroxide in the backward (negative) scan], or some continued minor structural reconstruction from the Faradaic redox reactions at much higher or much lower potential regimes.

Considering that the ETS signal in the double layer regime could be convoluted with residual redox reactions or structural relaxation originating from reactions outside this potential regime in the full potential range scan (0.05-1.40V vs. V_{RHE}), we narrowed our measurement potential range to only within the double layer region to avoid Faradaic redox reactions in the higher or lower potential regimes, thus eliminating possible interference from incomplete reaction/adsorption. Indeed, the ETS measurements in the pure double-layer region (0.40-0.60 V vs. V_{RHE}) reveal that the conductance is essentially flat without significant dependence on the potential (Fig. 1) c), confirming that there are no (or negligible) residue redox reactions within the narrowed potential window. This observation further confirms that the conductance of the PtNWs is not sensitive to electrochemical potential (instead only to surface adsorbates), consistent with previous studies. Additionally, control experiments conducted in the same device configuration without PtNWs show negligible conductance or conductance change compared to those with PtNWs (SI Appendix, Fig. S2), indicating the solution conductance has a negligible effect in our measurements.

Without the complication from the surface redox reaction, the measurement in the double layer region can allow us to probe the surface water protonation status at different pHs. The ETS measurements in the double regime in a series of solutions with pH values from 0 to 7 show that the ETS signal largely remains flat for each pH condition, but with distinct values at different pH (Fig. 1 c). Overall, the conductance of the PtNW device is clearly higher in acidic conditions (pH \sim 0-3) than in neutral (pH \sim 5-7) conditions, with a sharp decrease for pH values in-between. To further ensure that this change originates from the change in solution pH rather

than some irreversible change/drift in sample conductance, we conducted back-and-forth measurements from pH $1\rightarrow 4\rightarrow 7$ and then pH $7\rightarrow 4\rightarrow 1$, and achieved a highly consistent conductance change that does not depend on the measurement sequence, but only on the solution pH (SI Appendix, Fig. S3). These pH-dependent ETS signals indicate a clear change in surface water structure or protonation status as a function of pH.

The ETS response in the double layer region can be further utilized to obtain quantitative information related to the acidity of the Pt-water interface. By plotting the ETS conductance value versus solution pH (Fig. 1d), we obtain a trend closely resembling the protonation/deprotonation of a weak acid. In other words, the nearly constant ETS signal with high conductance at pH 1.0 - 3.0 indicates that there is little change in the protonation state of the interfacial water molecules in this pH range, suggesting a proton saturated (i.e., 'fully protonated') state. Similarly, the near-constant ETS signal with a low conductance value at pH 5.0 - 7.0 also indicates that there is little change in protonation states of interfacial water molecules in this regime, indicating a fully 'deprotonated' state.

Considering the Pt-surface hydronium (usually in the form of ${\rm H_3O^+}$ but may take other forms such as ${\rm H_5O_2^+}$ or more generally ${\rm H_{2y+1}O_y^+}$) as a weak acid (HA) that may deprotonate as:

$$Pt_{x} (H_{2y+1}O_{y})^{+} + H_{2}O \rightarrow Pt_{x} (H_{2}O)_{y} + H_{3}O^{+}$$
 [2]

we can write the protonation percentage as

$$y = \frac{[HA]}{[HA] + [A^-]} = \frac{1}{1 + \frac{K_a}{[H^+]}} = \frac{1}{1 + K_a * 10^{pH}}$$
 [3]

If we assume that the PtNWs with a fully protonated water surface has a constant conductance of G_p and the PtNWs with a fully deprotonated water surface have a constant conductance of G_{dp} , The ETS conductance signal can be fitted by the equation:

$$G_{\text{conductance}} = \frac{G_p - G_{dp}}{1 + K_a * 10^{pH}} + G_{dp}$$
 [4]

Importantly, this Henderson–Hasselbalch equation gives a nearly perfect fit, yielding $pK_a = 4.3$ with R^2 =0.995. This result suggests that hydronium adsorbed on Pt surface is indeed a weaker acid than bulk hydronium. That is, the Pt surface water molecules are more protonated than bulk water molecules.

To mimic pH 0 formally in the AIMD simulations, one ${\rm H_3O^+}$ molecule is included explicitly with 54 ${\rm H_2O}$ molecules. Without an explicit counter ion (ClO $_4^-$ in the experiment), the additional electron enters into the Pt electrode, increasing the work function to 4.51, which corresponds to an applied voltage of 0.07 V, close to the experiment HER onset potential. Thus, we can simulate both the pH and applied voltage in the experiment with a single ${\rm H_3O^+}$. The absence of the anion has a negligible effect, given that the ClO $_4^-$ do not normally absorb strongly on the surface and do not bind to ${\rm H_2O}$.

Reactive Molecular Dynamics Simulations

To predict the Pt-surface hydronium pK_a from the first principles, we carried out atomistic-based simulations to predict the distribution of H_3O^+ near Pt surfaces. We applied density functional theory (DFT) at the level of PBE-D3 (see Method section for detailed computational methods), which has been confirmed to provide accurate predictions (to ~ 0.05 eV) at affordable computational costs for electrochemical simulations, including oxygen reduction reactions (ORR) (40, 41), oxygen evolution reactions (OER)(42, 43), hydrogen evolution reactions (HOR) (44, 45), hydrogen oxidation reactions (HOR) (46), and CO_2 reduction reactions (CO2RR) (47–49).

We focus first on the two major exposed surfaces of the PtNWs, Pt(111) and Pt(100) (SI Appendix, Fig. S4). We describe the Pt-water interface using a 3-layer 3×4 slab with 36 Pt atoms, exposing either the (111) or (100) surface, combined with a water slab containing 55 H₂O molecules (~8 to 9 layers) plus one extra proton (H⁺) (1M concentration) (Fig. 2a, b). The extra proton was initially placed on waters in each of the eight layers above the Pt surface (~ 3 Å to ~ 12 Å from the Pt surface). Interestingly, in all cases, the H⁺ on the H₃O⁺ spontaneously migrates to the first layer via a Grotthuss hopping mechanism within 5 ps of MD equilibrium, indicating that H⁺ is thermodynamically most stable on the surface (i.e., the surface hydronium has a higher pK_a than bulk hydronium). We carried out the two-phase thermodynamics (2PT) analysis (50-52) of the velocity autocorrelation from the DFT-MD trajectory to predict entropy that together with enthalpy from MD leads to the free energy of the surface hydroniums, yielding a pK_a = 2.45 on Pt(111) and 2.58 on Pt(100) using the bulk electrolyte as reference (see SI Appendix, Table S1 and S2).

To more closely mimic the experimental PtNW structure, we further conducted reactive dynamics using a reactive force field (ReaxFF) (53, 54) by constructing a ~ 2 nm diameter and 2.23 nm long periodic PtNW immersed into a 1M HClO₄ electrolyte containing 3061 water and 60 H₃O⁺ per periodic cell (Fig. 2c). To this end, we first validated the accuracy of the ReaxFF predictions by applying ReaxFF to calculate the pK_a of surface hydronium on Pt(111) and Pt(100) separately and compared with those obtained from DFT-MD calculations. The ReaxFF-MD calculations give a p $K_a = 2.97$ on Pt(111), and $pK_a = 3.04$ on Pt(100), which are comparable with and only ~ 0.5 units higher (an error of 0.03 eV in the free energy) than those obtained in the DFT-MD calculations described above. The validation studies demonstrate that ReaxFF gives a comparable accuracy to DFT calculation, offering a pathway to evaluating H₃O⁺ distribution and the pK_a on realistic PtNW surface through the much larger scale ReaxFF simulation.

The 10,000-atom scale ReaxFF simulations of the realistic PtNWs show clearly the enrichment of $\rm H_3O^+$ near the Pt surface, as highlighted in the instantaneous atomic snapshots at 1 nanosecond (Fig. 2d and SI Appendix, Fig. S5). An average of 10,000 snapshots (200 snapshots for each of 50 independent simulations) further provides a statistical distribution of $\rm H_3O^+$ in the simulation cell (Fig. 2e), showing clear enrichment of $\rm H_3O^+$ on the PtNW-surface that quickly decays to the bulk concentration within \sim 1 nm from the surface (2-3 water layers). Lastly, the ReaxFF free energy calculations give an average pK_a = 3.82 for the $\rm H_3O^+$ in the first monolayer on the PtNW surface, which is consistent with the experimental value

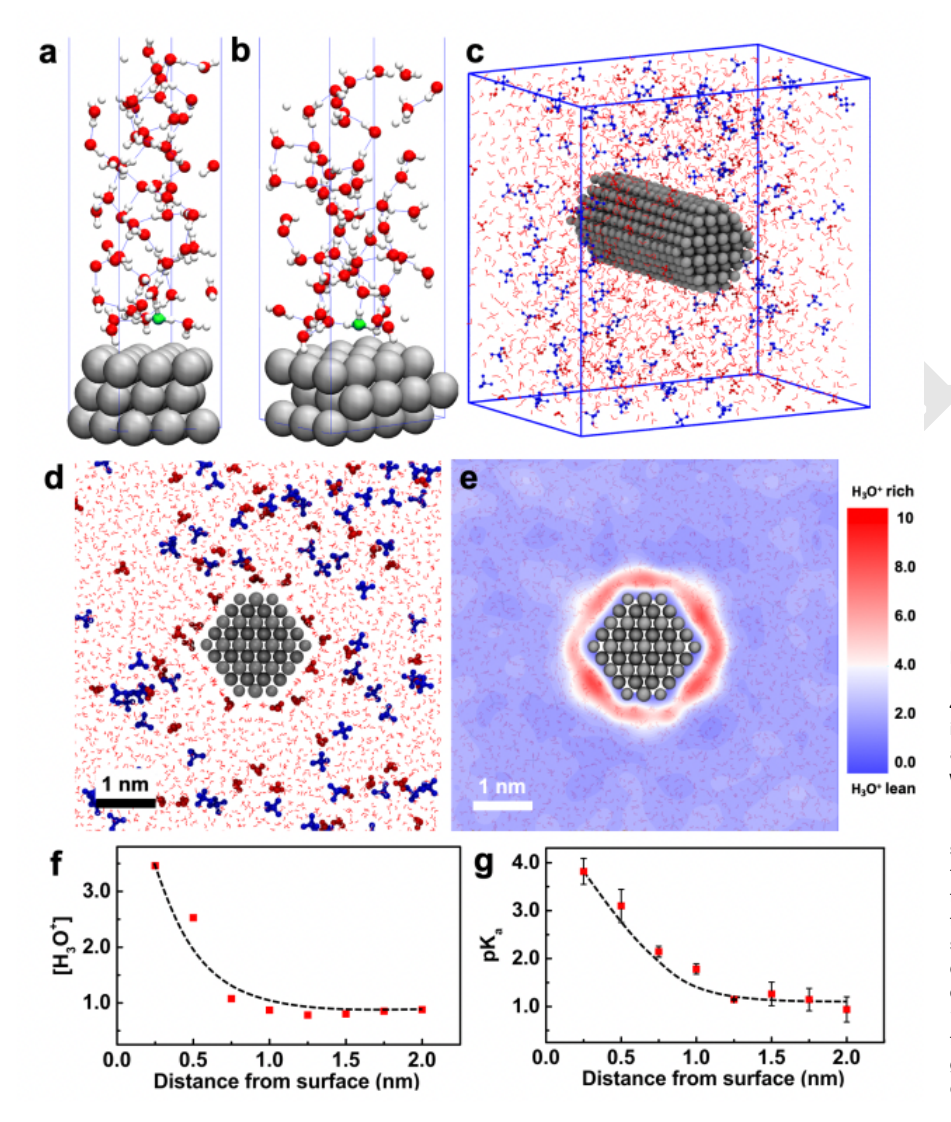


Fig. 2. QM and ReaxFF calculations of platinum-H₃O⁺ structure. a, Pt(111)/water interface for a 3 by 4 unit cell with one proton and 55 $\mbox{\rm H}_2\mbox{\rm O},$ one of which is protonated (green). b, Pt(100)/water interface for a 3 by 4 unit cell with one proton and 55 $\ensuremath{\text{H}_2\text{O}},$ one of which is protonated (green). c, Scheme of the PtNW ReaxFF MD simulation with 60 HClO₄ and 3061 $\mbox{H}_2\mbox{O}$ in a 6.63x6.63x2.23 \mbox{nm}^3 cell. The scheme shows a replica of 3 times in z-direction (PtNW axis) for viewing convenience. d, Snapshot of one simulation at 1 ns projected along the z-direction showing the instantaneous enrichment of H₃O⁺ near PtNW surface. (${\rm H_3O^+}$: in red, ${\rm CIO_4^-}$: blue). e, The statistical distribution of H₃O⁺ averaged from 50 independent ReaxFF MD simulations, each averaged over 100 snapshots. f, $H_3\mathrm{O}^+$ concentration versus distance showing clear enrichment on PtNW surface. g, Average pK_a versus distance showing significant enhancement of pK_a on PtNW surface.

Huang, Goddard, Duan et al. PNAS | **August 11, 2022** | vol. XXX | no. XX | **5**

 $(pK_a=4.3)$ determined from the ETS studies. Evaluation of the p K_a values for H_3O^+ at different distances from the Pt surface shows that the pK_a drops steeply as the hydronium is farther away from the Pt surface (Fig. 2g), which is consistent with the notably enhanced hydronium density near the Pt surface (Fig. 2f). Thus, both QM and ReaxFF calculations confirm the stabilization of H₃O⁺ on the Pt surface, leading to the notably increased p K_a . The enrichment of H_3O^+ (i.e., increase of pK_a) near Pt/water interface has been suggested in previous molecular dynamic simulations as well. (32) At the molecular level, surface adsorbed H₂O molecules predominantly have hydrogen pointing toward the Pt surface, with the exposed oxygen atoms behavior as hydrogen bond acceptors. This could lead to an enrichment of H₃O⁺ due to their enhanced ability (vs. H₂O) to donate hydrogen bond to the surface adsorbed water layer. The enrichment of H₃O⁺ near the Pt surface can correspondingly promote the protonation status of the surface adsorbed water, as revealed in our ETS measurement.

Our experimental studies provide a highly specific approach direct monitor of the surface protonation/deprotonation status to quantitatively determine the surface pK_a value for the first time. The close agreement between our ETS measurements and the DFT/ReaxFF calculations gives strong validation of the increased hydronium pK_a on the Pt surface from both the experimental and theoretical perspectives. We note that a previous study indicated that the potential of zero total charge (pztc) changes notably above pH 3.4 for the Pt(111) surface(55), suggesting a significant change in surface water structure at this point. This is likely due to the substantial change in protonation status in this pH regime found in our studies.

Correlating Surface Protonation Status with HER Kinetics

The Pt-surface adsorbed hydronium may have important mechanistic consequences for relevant electrochemical reactions, including HER and water electrolysis (56, 57). It has been well documented that HER kinetics depend on the solution pH (46, 57). Although there have been some general interpretations of such pH-dependence behavior, the fundamental reasons underlying these differences and a precise interpretation of the exact pH dependence remain a topic of considerable debate (13, 58). With our determination of the surface hydronium pK_a , we hypothesize that surface protonation status plays a fundamental role in HER, leading to distinct kinetics. Thus, we compared the HER kinetics with the Pt-surface hydronium pK_a. Indeed, the polarization curves for PtNW catalyzed HER show highly distinct behavior at different pH (Fig. 3a). In particular, for pH < 4.0, appreciable cathodic HER current can be observed near 0 V_{RHE} . On the other hand, when pH is > 4.5, the cathodic HER current observed near 0 V_{RHE} is almost negligible (still discernable using the logarithm scale shown in Fig. 3b), and appreciable HER current can be observed only at a much more negative potential (\sim -0.2 V_{RHE}). In the intermediate pH regime (pH 3.0-4.0), we observe a diffusion-limited current plateau, followed by another monotonic increase in reduction current at potentials more negative than -0.2 V vs. V_{RHE} . Based on the logarithmic plot of the polarization curve (Fig. 3b), we can derive the Tafel slopes for the HER reaction at different pH. Interestingly, the pH-dependent Tafel slopes also display a sharp transition around pH = 4, showing a low value of ~ 30 mV/decade at pH < 3 and a much higher value of ~ 120 mV/decade at pH > 5, suggesting distinct reaction pathways.

These observations, consistent with previous reports (59), can be explained by two distinct HER reaction pathways resulting from different surface water protonation status, local hydronium concentration, and diffusion of hydronium to the surface from the bulk. It is well known that the HER reaction follows three basic steps, with distinct rate-determining steps:

$$H_3O^+ + e^- \rightarrow H_{ad} + H_2O$$
 Volmer Step [5] 421

$$H_{ad} + H_3O^+ + e^- \rightarrow H_2 + H_2O$$
 Heyrovsky Step [6] 422

$$2H_{\rm ad} \rightarrow H_2$$
 Tafel Step [7] 423

in a cidic conditions where there are sufficient hydroniums as proton source for hydrogen adsorption; or

$$H_2O + e^- \rightarrow H_{ad} + OH^-$$
 Volmer Step [8] 426

$$H_{ad} + H_2O + e^- \rightarrow H_2 + OH^-$$
 Heyrovsky Step [9]

in more basic conditions where water becomes the major surface species to supply protons for hydrogen adsorption (60). Assuming an electron-transfer coefficient $\alpha=0.5$ and constant surface coverage, the Tafel slope of the reaction would be 30, 40, or 120 mV/decade depending on whether the rate-determining step is the Tafel, Heyrovsky, or Volmer step (13, 61, 62).

It is generally recognized that the Tafel step is rate-determining in acidic conditions, with an ideal Tafel slope of 30 mV/decade. On the other hand, for more basic conditions, the Volmer step becomes rate-determining, leading to a higher Tafel slope of 120 mV/decade. Although such distinctions in the reaction mechanism for acidic or basic conditions are generally accepted by the community, the exact transition between these two reaction mechanisms at intermediate pH and a molecular-level interpretation of such transition is elusive and a topic of considerable debate. Importantly, our determination of the surface pK $_a$ well explains such transitions in the reaction pathways and the corresponding switch of the Tafel slope in terms of the surface protonation status:

- (1) At solution pH 0-2, well below the surface pK_a , there are abundant protonated surface hydroniums as proton source for hydrogen adsorption. Thus, the reaction follows the typical acidic pathway with the Tafel step as the rate-determining step and a Tafel slope of 30 mV/decade;
- (2) At solution pH 5-7, well above the surface pK_a , the surface hydroniums are fully deprotonated with water molecules as the dominant species to supply protons; thus, the Volmer step becomes rate-determining, resulting in a large Tafel slope of 120 mV/decade;

Thus, the determined surface hydronium pK_a gives a robust molecular-level explanation of the switch of in the reaction mechanism at different pH and potential. At low overpotential, when the HER current is low, the limited supply of hydroniums at intermediate pH can satisfy a Tafel-step (pH \leq 2) or Heyrovsky-step (pH \leq 4) limited reaction pathway in the small current regime until reaching diffusion limitations that

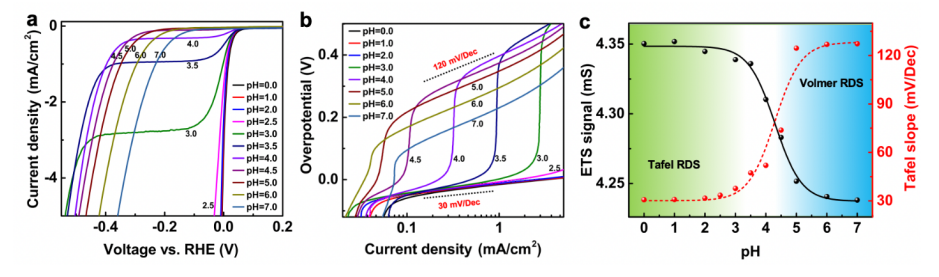


Fig. 3. Hydrogen evolution reaction kinetics on Pt. a, Hydrogen evolution reaction (HER) polarization curves of PtNWs on a rotating disk electrode (RDE) at different pH at constant ionic strength (0.10 M) b, HER overpotential vs. log current density, black dashed lines indicate the reference Tafel slope of 30 and 120 mV/dec. c, Tafel slopes measured for the HER in the pH range of 0 to 7 compared with the ETS signal, showing a fast Tafel-step limited kinetics with a Tafel slope of 30 mV/decade at lower pH, and Volmer-step limited kinetics with a much higher Tafel slope of 120 mV/decade at higher pH.

514

515

516

520

522

524

525

527

528

529

530

531

532

533

534

535

536

537

538

539

540

541

542

543

544

545

546

547

548

549

550

551

552

553

554

555

556

557

558

559

560

561

562

563

564

565

566

567

569

573

575

576

578

579

exhaust all local hydroniums. Beyond this plateau, all surface hydroniums are depleted, and the Volmer step becomes rate limiting, showing a Tafel slope of 120 mV/decade as the overpotential is further increased. We also note, with such a diffusion limitation at intermediate pH, the Tafel slope cannot be simply read out from the logarithmic plot. Instead, the value of the diffusion-limited current plateau was further utilized to deconvolute the impact of diffusion limitations to more accurately derive the Tafel slope in this regime (see Method and SI Appendix, Fig. S6).

Conclusion

465

466

467

468

469

470

471

473

474

476

477

478

479

480

481

482

484

485

486

487

488

489

492

493

494

495

498

499

500

501

502

503

505

506

507

508

509

510

511

512

We have used a unique surface adsorption-specific electrical transport spectroscopy (ETS) approach to investigate water structure and protonation status at Pt surfaces. With exclusively surface-specific signals, we were able to probe the surface water protonation status under a controlled potential range at various pH, for the first time, quantitatively determining the Pt-surface hydronium pK_a of 4.3. The QM-MD molecular dynamics calculations on Pt(100) and Pt(111) surface and the ReaxFF reactive molecular dynamics simulations on the PtNW confirm the hydronium enrichment near Pt surface and corroborate a surface hydronium pK_a of 2.5 to 4.4. Furthermore, we showed that the observed surface hydronium pK_a correlates well with pH-dependent HER kinetics: with the protonated surface states at lower pH favoring faster kinetics with a Tafel slope of 30 mV/dec, and the deprotonated states showing slower kinetics and a much higher Tafel slope of 120 mV/dec limited by hydrogen adsorption step. This excellent correlation offers a robust molecular level interpretation of the long-debated pH-dependent HER kinetics on Pt surface for the first time.

Our studies provide molecular insights into pH effects on the surface water structure and their critical role in the relevant electrochemical reactions. These results suggest further studies to fully understand the implications of our model on electrocatalysis on various relevant reactions. Since a water molecule can act as a base or an acid, further deprotonation of the Pt-water interface is quite possible and worthy of serious examination.

ACKNOWLEDGMENTS. X.D. acknowledges support from the National Science Foundation award 1800580. Y.H. acknowledges support from the Office of Naval Research by the grant number of N000141812155. W.A.G. received support from the Liquid Sunlight Alliance, which is supported by the U.S. Department of Energy, Office of Science, Office of Basic Energy Sciences, Fuels from Sunlight Hub under Award Number DE-SC0021266. T.C. thanks the support from the National Natural Science Foundation of China (21903058 and 22173066), the Natural Science Foundation of Jiangsu Higher Education Institutions (BK20190810), the Priority Academic

Program Development of Jiangsu Higher Education Institutions (PAPD), and partial support from the Collaborative Innovation Center of Suzhou NanoScience & Technology. Portions of this paper were used in the PhD thesis of G. Z.

- ZW Seh, et al., Combining theory and experiment in electrocatalysis: Insights into materials design. Science 355, eaad4998 (2017).
- VR Stamenkovic, D Strmcnik, PP Lopes, NM Markovic, Energy and fuels from electrochemical interfaces. Nat. Mater. 16, 57–69 (2017).
- L Li, P Wang, Q Shao, X Huang, Metallic nanostructures with low dimensionality for electrochemical water splitting. Chem. Soc. Rev. 49, 3072

 –3106 (2020).
- N Dubouis, A Grimaud, The hydrogen evolution reaction: from material to interfacial descriptors. Chem. Sci. 10, 9165–9181 (2019).
- I Ledezma-Yanez, et al., Interfacial water reorganization as a pH-dependent descriptor of the hydrogen evolution rate on platinum electrodes. Nat. Energy 2, 17031 (2017).
- S Ardo, et al., Pathways to electrochemical solar-hydrogen technologies. Energy & Environ. Sci. 11, 2768–2783 (2018).
- JJ Velasco-Velez, et al., The structure of interfacial water on gold electrodes studied by x-ray absorption spectroscopy. Science 346, 831–834 (2014).
- MF Toney, et al., Voltage-dependent ordering of water molecules at an electrode-electrolyte interface. Nature 368, 444-446 (1994).
- Ki Ataka, T Yotsuyanagi, M Osawa, Potential-Dependent Reorientation of Water Molecules at an Electrode/Electrolyte Interface Studied by Surface-Enhanced Infrared Absorption Spectroscopy. The J. Phys. Chem. 100, 10664–10672 (1996).
- YJ Zhang, ZF Su, JF Li, J Lipkowski, What Vibrational Spectroscopy Tells about Water Structure at the Electrified Palladium–Water Interface. The J. Phys. Chem. C 124, 13240–13248 (2020).
- AM Gardner, KH Saeed, AJ Cowan, Vibrational sum-frequency generation spectroscopy of electrode surfaces: studying the mechanisms of sustainable fuel generation and utilisation. *Phys. Chem. Chem. Phys.* 21, 12067–12086 (2019).
- CY Li, et al., In situ probing electrified interfacial water structures at atomically flat surfaces. Nat. Mater. 18, 697–701 (2019).
- Q Jia, E Liu, L Jiao, J Li, S Mukerjee, Current understandings of the sluggish kinetics of the hydrogen evolution and oxidation reactions in base. *Curr. Opin. Electrochem.* 12, 209–217 (2018).
- J Zheng, W Sheng, Z Zhuang, B Xu, Y Yan, Universal dependence of hydrogen oxidation and evolution reaction activity of platinum-group metals on pH and hydrogen binding energy. Sci. Adv. 2, e1501602 (2016).
- N Govindarajan, A Xu, K Chan, How pH affects electrochemical processes. Science 375, 379–380 (2022).
- E Liu, et al., Interfacial water shuffling the intermediates of hydrogen oxidation and evolution reactions in aqueous media. Energy & Environ. Sci. 13, 3064–3074 (2020).
- AM Darlington, et al., Separating the pH-Dependent Behavior of Water in the Stern and Diffuse Layers with Varying Salt Concentration. The J. Phys. Chem. C 121, 20229–20241 (2017)
- V Briega-Martos, E Herrero, JM Feliu, Effect of pH and Water Structure on the Oxygen Reduction Reaction on platinum electrodes. *Electrochimica Acta* 241, 497–509 (2017).
- D Strmcnik, et al., Improving the hydrogen oxidation reaction rate by promotion of hydroxyl adsorption. Nat. Chem. 5, 300–306 (2013).
- PS Lamoureux, AR Singh, K Chan, pH Effects on Hydrogen Evolution and Oxidation over Pt(111): Insights from First-Principles. ACS Catal. 9, 6194–6201 (2019).
- FT Wagner, TE Moylan, Generation of surface hydronium from water and hydrogen coad sorbed on Pt(111). Surf. Sci. 206, 187–202 (1988).
- Y Shingaya, M Ito, Coordination number and molecular orientation of hydronium cation/bisulfate anion adlayers on Pt(111). Surf. Sci. 368, 318–323 (1996).
- K Hirota, MB Song, M Ito, In-situ infrared spectroscopy of water and electrolytes adsorbed on a Pt(111) electrode surface in acid solution. Structural changes of adsorbed water molecules upon an electrode potential. Chem. Phys. Lett. 250, 335–341 (1996).
- M Dunwell, Y Yan, B Xu, A surface-enhanced infrared absorption spectroscopic study of pH dependent water adsorption on Au. Surf. Sci. 650, 51–56 (2016).
- P Paredes Olivera, A Ferral, EM Patrito, Theoretical Investigation of Hydrated Hydronium Ions on Aq(111). The J. Phys. Chem. B 105, 7227–7238 (2001).
- M Otani, et al., Structure of the water/platinum interface—a first principles simulation under bias potential. Phys. Chem. Chem. Phys. 10, 3609 (2008).
- J Rossmeisl, E Skúlason, ME Björketun, V Tripkovic, JK Nørskov, Modeling the electrified solid-liquid interface. Chem. Phys. Lett. 466, 68–71 (2008).
- MH Hansen, A Nilsson, J Rossmeisl, Modelling pH and potential in dynamic structures of the water/Pt(111) interface on the atomic scale. Phys. Chem. Chem. Phys. 19, 23505–23514

580 (2017).

581

582

583

584

585 586

591

592

593

594

595

596 597

598 599

600

- PS Rice, Y Mao, C Guo, P Hu, Interconversion of hydrated protons at the interface between 29. liquid water and platinum. Phys. Chem. Chem. Phys. 21, 5932-5940 (2019).
- V Buch, A Milet, R Vácha, P Jungwirth, JP Devlin, Water surface is acidic. Proc. Natl. Acad. 30. Sci. 104, 7342-7347 (2007).
- DT Limmer, AP Willard, P Madden, D Chandler, Hydration of metal surfaces can be dynamically heterogeneous and hydrophobic. Proc. Natl. Acad. Sci. 110, 4200-4205 (2013).
- 587 P Brüesch, T Christen, The electric double layer at a metal electrode in pure water. J. Appl. 588 Phys. 95, 2846-2856 (2004).
- 589 L Braunwarth, C Jung, T Jacob, Exploring the Structure-Activity Relationship on Platinum 590 Nanoparticles. Top. Catal. 63, 1647-1657 (2020).
 - H Wang, et al., Electrochemical tuning of vertically aligned MoS $_{\mathrm{2}}$ nanofilms and its application in improving hydrogen evolution reaction. Proc. Natl. Acad. Sci. 110, 19701-19706 (2013).
 - 35 M Ding, et al., An on-chip electrical transport spectroscopy approach for in situ monitoring electrochemical interfaces. Nat. Commun. 6, 7867 (2015).
 - M Ding, et al., On-Chip in Situ Monitoring of Competitive Interfacial Anionic Chemisorption as a Descriptor for Oxygen Reduction Kinetics. ACS Cent. Sci. 4, 590-599 (2018).
 - 37 EH Sondheimer, The mean free path of electrons in metals. Adv. Phys. 50, 499-537 (2001).
 - M Ding, et al., Highly Sensitive Chemical Detection with Tunable Sensitivity and Selectivity from Ultrathin Platinum Nanowires. Small 13, 1602969 (2017).
- F Yang, KC Donavan, SC Kung, RM Penner, The Surface Scattering-Based Detection of 601 602 Hydrogen in Air Using a Platinum Nanowire. Nano Lett. 12, 2924-2930 (2012).
- 603 T Cheng, et al., Mechanism and kinetics of the electrocatalytic reaction responsible for the 604 high cost of hydrogen fuel cells. Phys. Chem. Chem. Phys. 19, 2666-2673 (2017).
- Y Chen, T Cheng, WA Goddard III, Atomistic Explanation of the Dramatically Improved Oxy-605 gen Reduction Reaction of Jagged Platinum Nanowires, 50 Times Better than Pt. J. Am. 606 Chem. Soc. 142, 8625-8632 (2020). 607
- 608 42. H Xiao, H Shin, WA Goddard, Synergy between Fe and Ni in the optimal performance of 609 (Ni,Fe)OOH catalysts for the oxygen evolution reaction. Proc. Natl. Acad. Sci. 115, 5872-610
- 611 43. C Liu, et al., Oxygen evolution reaction over catalytic single-site Co in a well-defined brookite TiO2 nanorod surface. Nat. Catal. 4, 36-45 (2021). 612
- 613 Y Huang, RJ Nielsen, WA Goddard, MP Soriaga, The Reaction Mechanism with Free Energy 614 Barriers for Electrochemical Dihydrogen Evolution on MoS 2. J. Am. Chem. Soc. 137, 6692-615 6698 (2015)
- 616 Y Huang, RJ Nielsen, WA Goddard, Reaction Mechanism for the Hydrogen Evolution Re-617 action on the Basal Plane Sulfur Vacancy Site of MoS 2 Using Grand Canonical Potential Kinetics. J. Am. Chem. Soc. 140, 16773-16782 (2018). 618
- T Cheng, L Wang, BV Merinov, WA Goddard, Explanation of Dramatic pH-Dependence of 619 Hydrogen Binding on Noble Metal Electrode: Greatly Weakened Water Adsorption at High 620 pH. J. Am. Chem. Soc. 140, 7787-7790 (2018). 621
- 47. H Xiao, T Cheng, WA Goddard, R Sundararaman, Mechanistic Explanation of the pH Depen-622 623 dence and Onset Potentials for Hydrocarbon Products from Electrochemical Reduction of CO on Cu (111). J. Am. Chem. Soc. 138, 483-486 (2016). 624
- 48. T Cheng, H Xiao, WA Goddard, Full atomistic reaction mechanism with kinetics for CO reduc-625 tion on Cu(100) from ab initio molecular dynamics free-energy calculations at 298 K. Proc. 626 Natl. Acad. Sci. 114, 1795-1800 (2017). 627
- 49. H Xiao, T Cheng, WA Goddard, Atomistic Mechanisms Underlying Selectivities in C 1 and 628 C 2 Products from Electrochemical Reduction of CO on Cu(111), J. Am. Chem. Soc. 139. 629 630 130-136 (2017).
- 631 ST Lin, M Blanco, WA Goddard. The two-phase model for calculating thermodynamic proper-632 ties of liquids from molecular dynamics: Validation for the phase diagram of Lennard-Jones 633 fluids. The J. Chem. Phys. 119, 11792-11805 (2003).
- ST Lin, PK Maiti, WA Goddard, Two-Phase Thermodynamic Model for Efficient and Accurate 634 635 Absolute Entropy of Water from Molecular Dynamics Simulations. The J. Phys. Chem. B 114, 636 8191-8198 (2010).
- 52. TA Pascal, ST Lin, WA Goddard III, Thermodynamics of liquids; standard molar entropies 637 and heat capacities of common solvents from 2PT molecular dynamics. Phys. Chem. Chem. 638 639 Phys. 13, 169-181 (2011).
- 640 53. ACT van Duin, S Dasgupta, F Lorant, WA Goddard, ReaxFF: A Reactive Force Field for 641 Hydrocarbons. The J. Phys. Chem. A 105, 9396-9409 (2001).
- 642 Y Kim, C Noh, Y Jung, H Kang, The Nature of Hydrated Protons on Platinum Surfaces. Chem. 643 A Eur. J. 23, 17566-17575 (2017)
- 644 55. R Rizo, E Sitta, E Herrero, V Climent, JM Feliu, Towards the understanding of the interfacial 645 pH scale at Pt(1 1 1) electrodes. Electrochimica Acta 162, 138-145 (2015).
 - W Sheng, HA Gasteiger, Y Shao-Horn, Hydrogen Oxidation and Evolution Reaction Kinetics on Platinum: Acid vs Alkaline Electrolytes. J. The Electrochem. Soc. 157, B1529 (2010).
 - 57. Y Zheng, Y Jiao, A Vasileff, S Qiao, The Hydrogen Evolution Reaction in Alkaline Solution: From Theory, Single Crystal Models, to Practical Electrocatalysts. Angewandte Chemie Int. Ed. 57, 7568-7579 (2018).
- 651 T Shinagawa, AT Garcia-Esparza, K Takanabe, Mechanistic Switching by Hydronium Ion Activity for Hydrogen Evolution and Oxidation over Polycrystalline Platinum Disk and Plat-652 inum/Carbon Electrodes. ChemElectroChem 1, 1497-1507 (2014). 653
- 654 MC Banta, N Hackerman, The Effect of Acidity on the Differential Capacity of Polarized Plat-655 inum Electrodes. J. The Electrochem. Soc. 111, 114 (1964).
- 656 NM Marković, BN Grgur, PN Ross, Temperature-Dependent Hydrogen Electrochemistry on Platinum Low-Index Single-Crystal Surfaces in Acid Solutions. The J. Phys. Chem. B 101, 657 658 5405-5413 (1997).
- 61. B Conway, L Bai, Determination of adsorption of OPD H species in the cathodic hydrogen 659 660 evolution reaction at Pt in relation to electrocatalysis. J. Electroanal. Chem. Interfacial Elec 661 trochem. 198, 149-175 (1986).
- 662 Y Koutetskiia, V Levich, The use of a rotating disc electrode for studying kinetic and catalytic 663 processes in electrochemistry. Dokl. Akad. Nauk SSSR 117, 441-444 (1957).

646

647

648

649 650